Proceedings of the 2005 IEEE
Engineering in Medicine and Biology 27th Annual Conference
Shanghai, China, September 1-4, 2005

A Simple Cycle-Averaged Model for Cardiovascular Dynamics

Tushar A. Parlikar and George C. Verghese
Laboratory for Electromagnetic and Electronic Systems
Massachusetts Institute of Technology, Room 10-015, Cambridge, Massachusetts 02139
Telephone: (617) 253–0207; Fax: (617) 258–6774; Email: parlikar@mit.edu

Abstract— **Lumped-parameter time-varying electrical circuit analogs for cardiovascular systems are frequently used in computational models for simulating and analyzing hemodynamics. These pulsatile models provide details of the beat-by-beat or *intra*cycle dynamics. In other settings, however, such as when tracking a hospital patient's hemodynamic state over time, it is more useful to track trends in the *inter*cycle dynamics. In this paper, we apply a cycle-averaging method to a simple pulsatile cardiovascular model to derive a cycle-averaged model for cardiovascular dynamics. The resulting cycle-averaged model captures the intercycle dynamics with relatively small approximation errors for a large range of perturbations in parameters such as systemic vascular resistance.**

I. Introduction

The goal of this paper is to study a cycle-averaged model for cardiovascular dynamics, derived from a simple pulsatile cardiovascular model. *Pulsatile* models of the cardiovascular system have been used since the 1960s in both teaching and research, and capture the temporal features of the heart's pumping action during the cardiac cycle.

Cycle-averaged models, on the other hand, are effective in representing dynamics that occur over longer time scales, and are much used in fields such as power electronics [1]. In these models, only the short-term cycle-averages (i.e., averages over one cycle) of the relevant variables are tracked, instead of their intracycle variations. Such models are normally more computationally efficient than their pulsatile counterparts because the details of the waveforms within each cycle are ignored.

Figure 1 shows the pulsatile arterial blood pressure (ABP) and left ventricular pressure (LVP) waveforms, along with their calculated cycle-averages from a simulation of a pulsatile model of the cardiovascular system. In order to capture the transient changes in ABP or LVP, it would for many purposes suffice to capture their cycle-averages, and in order to represent these cycle-averages dynamically, we need a *cycle-averaged* model.

Previous work on cycle-averaged cardiovascular models (see [2]) used a piecewise constant ventricular elastance, which led to unrealistic waveforms in the pulsatile model. Furthermore, the cycle-averaged model was derived there in a less general way.

The outline of this paper is as follows. In Section II, we describe the simple pulsatile cardiovascular model to which we apply the cycle-averaging methodology. After giving some background on cycle-averaging methodology in Section III, we derive a cycle-averaged representation for the simple pulsatile cardiovascular model in Section IV. Simulation results obtained using this cycle-averaged model are presented and evaluated in Section V.

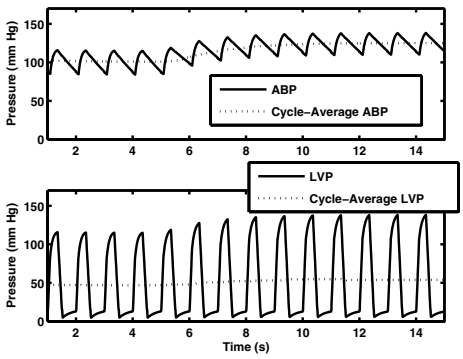

Fig. 1. Response of a pulsatile cardiovascular model to a step change in systemic vascular resistance.

II. Cardiovascular Circuit Models

One particularly convenient method of representing the cardiovascular system is to use lumped-parameter electrical circuit analogs for the different vascular segments. The electric circuit analogs for cardiovascular variables are: current I for flow, voltage V for pressure, ideal diodes D for heart valves, resistance R for valvular or vascular resistance to flow, charge Q for volume, inductance L for inertia, and capacitance C for compliance. Elastance, E, is defined as the inverse of capacitance or compliance. Circuit analogs for the ventricles in the heart and peripheral circulation compartments can easily be combined to create lumped-parameter cardiovascular circuit models, such as the cardiovascular simulator [3]. In this paper, we ignore the effects of inertia in the blood flow.

The model we propose here, the simple pulsatile cardiovascular model or the *pulsatile model* as we refer to it hereafter, has a single ventricular compartment. This model is justified for use mainly in simulating systemic vascular disease conditions such as hemorrhaging in the peripheral circulation. Figure 2 illustrates the circuit representation for the pulsatile model, where C_a is the arterial compliance, C_v is the venous compliance, $C_h(t)$ is the time-varying ventricular compliance, R_1 is the inflow resistance to the ventricle, R_2 is the outflow resistance from the ventricle, and R_3 is the total peripheral resistance. The voltage V_h is the

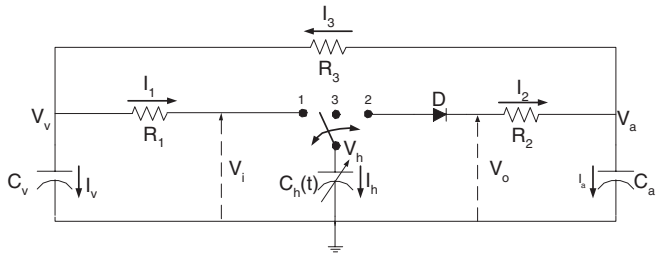

Fig. 2. The simple pulsatile cardiovascular model uses a 3-way switch which allows for simpler analysis of the circuit. V_i and V_o are defined here for future reference.

Parameter	Value in pulsatile model
R_1	0.01 mmHg/(ml/s)
R_2	0.03 mmHg/(ml/s)
R_3	1 mmHg/(ml/s)
C_a	2 mmHg/ml
C_v	100 mmHg/ml
E_d	0.1 ml/mmHg
E_s	2.5 ml/mmHg
$V_a(0)$	91.2281 mm Hg
$V_v(0)$	15.0337 mm Hg
$Q_h(0)$	127.383 mm Hg
T	1 s

TABLE I

SUMMARY OF PARAMETERS FOR THE PULSATILE MODEL.

ventricular pressure (VP), V_v is the central venous pressure (CVP), and V_a is the arterial blood pressure (ABP). The ventricular volume is Q_h.

The elastance function $E_h(t)$=$1/C_h(t)$ for the ventricle is represented as a piecewise linear function given by:

$$E_h(t) = \begin{cases} \frac{3(E_s-E_d)}{T}t + E_d & \text{for} \quad 0 \le t \le \frac{T}{3} \\ \frac{6(E_s-E_d)}{T}(\frac{T}{3} - t) + E_s & \text{for} \quad \frac{T}{3} \le t \le \frac{T}{2} \\ E_d & \text{for} \quad \frac{T}{2} \le t \le T \end{cases} \tag{1}$$

where T is the duration of the cardiac cycle, E_s is the end-systolic elastance, and E_d ($\ll E_s$) is the end-diastolic elastance. Such a time-varying elastance function approximates human data quite well [4].

The parameters used in the pulsatile model, including the initial conditions for our simulations, are shown in Table I. These parameters represent typical values for a 70 kg male human [5], and when used with (1), result in reasonable approximations of the pressure waveforms during the cardiac cycle.

We can define switching functions for the switch and diode in the pulsatile model. Figure 3 shows these switching functions for T=1 s, where: $s_1(t)$ equals 1 when the switch is in position 1, and 0 otherwise; $s_2(t)$ equals 1 when the switch is in position 2, and 0 otherwise; $s_3(t)$ equals 1 when the switch is in position 3, and 0 otherwise; and $s_D(t)$ equals 1 when the diode D is conducting (between t=t_D and t=$\frac{T}{3}$), and 0 otherwise.

The pulsatile model has four regions of operation, corresponding directly with the four periods of the cardiac cycle: contraction (I), ejection (II), expansion (III), and filling (IV), as shown in Fig. 4. The four regions are determined by the position of the switch and the state of the diode, as shown in Table II.

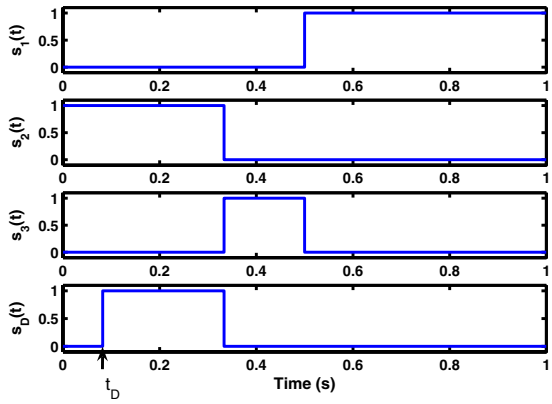

Fig. 3. Switching functions for the 3-way switch and diode in the pulsatile model for T=1 s.

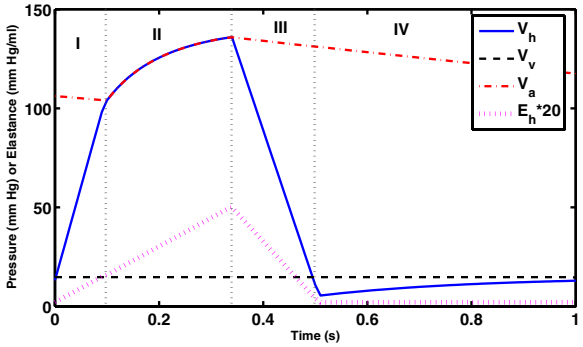

Fig. 4. Waveforms generated over a single cycle of the pulsatile model for T=1 s. This circuit has four regions of operation.

Region	Switch Position	Diode State
I (contraction)	2	Off
II (ejection)	2	On
III (expansion)	3	Off
IV (filling)	1	Off

TABLE II

DEFINITION OF THE 4 REGIONS IN THE PULSATILE MODEL.

With the switching functions described above, and with Q_h (=V_h/E_h), V_a and V_v as state variables[1], we have a state-space description for the pulsatile model given by:

$$\frac{dQ_h}{dt} = \frac{s_1(V_v - E_hQ_h)}{R_1} + \frac{s_D(V_a - E_hQ_h)}{R_2} \tag{2}$$

$$C_a\frac{dV_a}{dt} = \frac{s_D(E_hQ_h - V_a)}{R_2} + \frac{(V_v - V_a)}{R_3} \tag{3}$$

$$C_v\frac{dV_v}{dt} = \frac{s_1(E_hQ_h - V_v)}{R_1} + \frac{(V_a - V_v)}{R_3} \tag{4}$$

[1]Q_h is used as a state variable instead of V_h because it ensures smaller numerical errors as the term $\frac{dC_h}{dt}$ does not appear in the state-space model.

where the parameters p=$\{R_1, R_2, R_3, C_a, C_v\}$ are fixed, and we have dropped the time argument t for notational simplicity. More compactly, we can write:

$$\frac{d}{dt}\mathbf{x} = \mathcal{A}(s_1, s_D, p)\mathbf{x} \tag{5}$$

where $\mathbf{x}$ is the vector of state variables.

For realistic simulations involving many heart cycles, one would also have to wrap around this model the various feedback control mechanisms that regulate blood pressure, as done in [5]. However, since these mechanisms act on time scales of a heart cycle or longer, and since they typically use cycle-averaged, rather than instantaneous (or pulsatile), quantities as their inputs, it is not necessary to model them for purposes of deriving a cycle-averaged model. Instead, once a cycle-averaged model has been obtained, the various control loops can be wrapped around it.

III. Cycle-Averaging Techniques

In this section, we give some background on cycle-averaging techniques [6]. A signal $x(\cdot)$ has a complex Fourier series representation [7] on the interval $[t-T, t]$ that can be written as

$$x(\tau) = \sum_{k=-\infty}^{\infty} X_k(t) e^{jk\frac{2\pi}{T}\tau} \tag{6}$$

for $\tau \in [t-T, t]$. The $X_k(t)$ are the complex Fourier series coefficients, also referred to as the $index$-k averages and thus denoted by $\langle x \rangle_k(t)$. These complex coefficients are given by:

$$X_k(t) = \langle x \rangle_k(t) = \frac{1}{T}\int_{t-T}^{t} x(\tau) e^{-jk\frac{2\pi}{T}\tau}\, d\tau \tag{7}$$

thanks to the orthogonality properties of the basis functions $\{e^{-jk\frac{2\pi}{T}\tau}\}$ on an interval of length T. If $x(\cdot)$ were actually periodic with period T, then the $X_k(t)$ would be constants, independent of t. For waveforms that deviate only slowly and/or slightly from such periodicity, the $X_k(t)$ will have only slow and/or slight departures from constant values, and this fact can be exploited when making modeling approximations.

From (7), with k=0, we obtain the standard formula for the cycle-average of the variable $x(t)$, namely:

$$X_0(t) = \frac{1}{T}\int_{t-T}^{t} x(\tau)\, d\tau. \tag{8}$$

This index-0 cycle-average is simply the dc term in the Fourier series (6). It is also the short-term average of the variable $x(t)$ that we wish to track in our cycle-averaged models. In the cardiovascular circuit models where we apply these expressions, T is simply the length of the cardiac cycle.

By differentiating (7), we easily obtain an expression for the derivative of the index-k cycle-average:

$$\frac{d}{dt}X_k(t) = \frac{dx}{dt}_k - jk\frac{2\pi}{T}X_k(t)\ . \tag{9}$$

The index-k cycle-average of the product of two signals, $x(t)$ and $y(t)$, is given by the well-known and easily verified discrete convolution formula for the product of two polynomials [7]:

$$\langle xy \rangle_k = \sum_{m=-\infty}^{\infty} X_{k-m} Y_m \tag{10}$$

where we have dropped the time argument t from the expression for notational simplicity. If $x(t)$ or $y(t)$ can be approximated well by its index-0 cycle-average only (which is the case if it has low relative ripple[2]), (10) simply reduces to:

$$\langle xy \rangle_0 \approx X_0 Y_0\ . \tag{11}$$

The index-k cycle-average of the product of three signals, $x(t)$, $y(t)$, and $z(t)$, can be obtained by applying the discrete convolution relationship (10) to $(x(t)y(t))(z(t))$. To write real-valued expressions for the complex-valued expressions that result from using (10), we can use the fact that for any signal $x(t)$, X_k and X_{-k} are complex conjugates. Therefore:

$$X_k \;=\; X_k^R + jX_k^I = X_{-k}^* = (X_k^R - jX_k^I)^* \tag{12}$$

where R and I denote real and imaginary parts, and * denotes complex conjugation.

In our application, we can neglect many of the Fourier series coefficients, making both (10) and its extension to the product of three signals much simpler to apply. For example, assuming only the index-0 and index-1 cycle-averages are significant, we have that:

$$\langle xy \rangle_0 = X_0 Y_0 + 2(X_1^R Y_1^R + X_1^I Y_1^I)\ . \tag{13}$$

$$\langle xy \rangle_1^R = X_0 Y_1^R + X_1^R Y_0\ . \tag{14}$$

$$\langle xy \rangle_1^I = X_0 Y_1^I + X_1^I Y_0\ . \tag{15}$$

$$\langle xyz \rangle_0 = X_0\langle yz \rangle_0 + 2(X_1^R\langle yz \rangle_1^R + X_1^I\langle yz \rangle_I^I)\ . \tag{16}$$

$$\langle xyz \rangle_1^R = X_0\langle yz \rangle_1^R + X_1^R\langle yz \rangle_0 + X_1^R(X_1^R Y_1^R - X_1^I Y_1^I) - X_1^I(X_1^R Y_1^I + X_1^I Y_1^R)\ . \tag{17}$$

$$\langle xyz \rangle_1^I = X_0\langle yz \rangle_1^I + X_1^I\langle yz \rangle_0 + X_1^I(X_1^R Y_1^R - X_1^I Y_1^I) + X_1^R(X_1^R Y_1^I + X_1^I Y_1^R)\ . \tag{18}$$

To obtain a cycle-averaged model, one can simply apply the formulae derived in this section to a state-space model. Note that linear and time-invariant circuit elements, such as C_a and C_v, are not affected by the cycle-average operator. If we represent circuit variables by their index-0 and index-1 cycle-averages, but keep the index-1 cycle-averages constant, we end up with what we shall call an *index-0 cycle-averaged model*.

IV. The Index-0 Cycle-Averaged Model

To obtain an index-0 cycle-averaged model from the pulsatile model, we first need to approximately express the index-0 cycle-average S_{D0} of the switching function s_D for the diode D in terms of cycle-averages of V_a, Q_h, and V_v.

[2]Relative ripple is defined as the maximum peak-to-peak variation of a waveform divided by its average value.

Such an approximation can be obtained on examination of the relevant waveforms, and is given by:

$$S_{D0} = \frac{T}{3} - \frac{E_d}{3(E_s - E_d)}\left(\frac{V_{a0}}{V_{v0}} - 1\right). \qquad (19)$$

To derive an index-0 cycle-averaged model, one needs to find nominal values at which to fix the index-1 cycle averages, and justify that the index-2 and higher cycle-averages can be neglected. From simulations of the pulsatile model, we have justified the latter assumption. We then numerically calculated these index-1 cycle-averages using steady-state Fourier series representations of all the hemodynamic waveforms and switching functions from our simulations. The steady-state pulsatile model waveforms we used were obtained from simulations with the parameters in Table I. The results of this exercise are shown in Table III. Since $s_1(t)$ is half-wave symmetric, it has no index-m cycle-averages for m even ($m \geq 2$).

Variable	$\langle\bullet\rangle_0$	$\langle\bullet\rangle_1^R$	$\langle\bullet\rangle_1^I$	$\langle\bullet\rangle_2^R$	$\langle\bullet\rangle_2^I$
V_v	15.23	-0.0866	-0.0333	0.0179	0.0085
V_a	100.54	-4.908	-3.594	-1.912	0.8346
Q_h	88.12	18.477	10.518	2.033	-2.524
E_h	0.7000	-0.0912	-0.4738	-0.2052	0.1185
s_1	0.5000	0.0001	0.3183	–	–
s_D	0.2511	0.0592	-0.2180	-0.1373	-0.0805

TABLE III

VALUES FOR THE CYCLE-AVERAGES IN STEADY STATE.

Using the values listed in Table III and applying the cycle-average operators from the previous section to (2-4), we obtain an index-0 cycle-averaged model:

$$\frac{d}{dt}\mathbf{X}_0(t) = \frac{d}{dt}\begin{bmatrix} Q_{h0}(t) \\ V_{a0}(t) \\ V_{v0}(t) \end{bmatrix}$$

$$= \begin{bmatrix} -\frac{\langle s_1 E_h Q_h\rangle_0}{R_1} - \frac{\langle s_D E_h Q_h\rangle_0}{R_2} + \frac{\langle s_D V_a\rangle_0}{R_2} + \frac{\langle s_1 V_v\rangle_0}{R_1} \\ \frac{\langle s_D E_h Q_h\rangle_0}{R_1 C_a} - \frac{(R_2+R_3)V_{a0}}{R_2 R_3 C_a} + \frac{V_{v0}}{R_3 C_a} \\ \frac{\langle s_1 E_h Q_h\rangle_0}{R_1 C_v} + \frac{V_{a0}}{R_3 C_v} - \frac{\langle s_1 V_v\rangle_0}{R_1 C_v} - \frac{V_{v0}}{R_3 C_v} \end{bmatrix} \qquad (20)$$

where the time argument t has again been dropped from the last matrix for notational simplicity. Assuming that the index-0 cycle-averages are dynamic, that the index-1 cycle-averages are static, and that the index-2 or higher cycle-averages are negligible, we can rewrite (20), using (13)-(18), as:

$$\frac{d}{dt}\mathbf{X}_0(t) \approx \mathcal{C}(S_{10}, S_{D0}(t), p)\mathbf{X}_0(t) + \mathbf{d}(S_{11}, S_{D1}, \mathbf{X}_1, p) \qquad (21)$$

where $\mathcal{C}(S_{10}, S_{D0}(t), p)$ is dependent on the index-0 cycle-averages of the switching functions and the parameters p, and where $\mathbf{d}(S_{11}, S_{D1}, \mathbf{X}_1, p)$ is dependent on the index-1 cycle-averages of the switching functions, the index-1 cycle-averages $\mathbf{X}_1$, and the parameters p.

Note that for fixed values of period T and parameters p, $\mathbf{d}$ is constant. Furthermore, the state variables in this cycle-averaged model are the index-0 cycle-averages of the state variables in the pulsatile model. The total charge in this cycle-averaged circuit is the same as the total charge in the pulsatile model circuit.

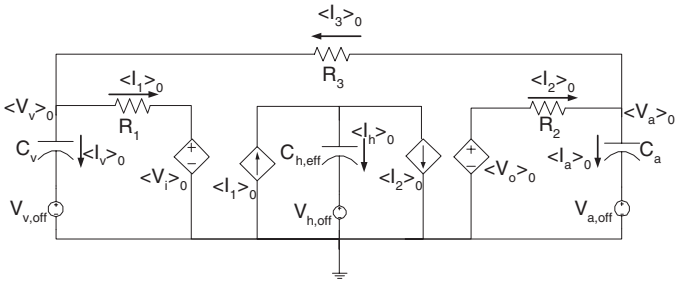

Fig. 5. Index-0 Cycle-Averaged Model with two-voltage dependent voltage sources and two current-dependent voltage sources.

Initially, the parameters p in $\mathcal{C}$ and $\mathbf{d}$ are set to the values that appear in Table I, which we shall call the parameter set p_{nom}. To start the cycle-averaged model in steady state, the initial conditions $\mathbf{X}_0(0)$ for the index-0 cycle-averaged model are set equal to the calculated cycle-averages of the steady-state (ss) simulated waveforms, $\mathbf{x}_{ss}$, of the pulsatile model using the parameters p_{nom}.

Due to truncation error in the Fourier series approximations leading to (21), however, setting $\mathbf{X}_0(0)$=$\mathbf{x}_{ss}$ in the index-0 cycle-averaged model leads to a non-zero value for $\mathcal{C}(S_{10}, S_{D0}(0), p_{nom})\mathbf{x}_{ss}$ + $\mathbf{d}(S_{11}, S_{D1}, \mathbf{X}_1, p_{nom})$ in the index-0 cycle-averaged model. This violates the assumption that the circuit starts in steady state. To correct for this truncation error, we can subtract a *fixed* correction term:

$$\mathbf{e} = \mathcal{C}(S_{10}, S_{D0}(0), p_{nom})\mathbf{x}_{ss} + \mathbf{d}(S_{11}, S_{D1}, \mathbf{X}_1, p_{nom}) \qquad (22)$$

from the right side of (21). The index-0 cycle-averaged model we propose is then given by:

$$\frac{d}{dt}\mathbf{X}_0(t) = \mathcal{C}(S_{10}, S_{D0}(t), p)\mathbf{X}_0(t) + \mathbf{d}(S_{11}, S_{D1}, \mathbf{X}_1, p) - \mathbf{e}. \qquad (23)$$

We can also construct a circuit model that captures the dynamics of the index-0 cycle-averaged model using voltage-dependent voltage sources and current-dependent current sources. Such an index-0 cycle-averaged circuit is shown in Fig. 5. In this circuit, the average compliance for the left ventricle, $C_{h,eff}$, is equal to $1/E_{h0}$ (see [2] for a derivation), and the sources $V_{v,off}$, $V_{h,off}$, and $V_{a,off}$ are introduced to take the correction term $\mathbf{e}$ in (23) into account. Using V_i and V_o from the circuit in Fig. 2, we can write:

$$V_{i0} = S_{10}V_{h0} + (1 - S_{10})V_{v0} + K_i \qquad (24)$$

$$V_{o0} = S_{D0}V_{h0} + (1 - S_{D0})V_{a0} + K_o \qquad (25)$$

where K_i and K_o are constants that are introduced from the (fixed) index-1 cycle-averages of s_D, V_h, V_a, and V_v.

V. RESULTS AND DISCUSSION

Using the index-0 cycle-averaged model (23), we obtained simulation results from a typical transient response to step changes in R_3, the systemic vascular resistance. Figure 6 shows the transient responses of the index-0 cycle-averaged

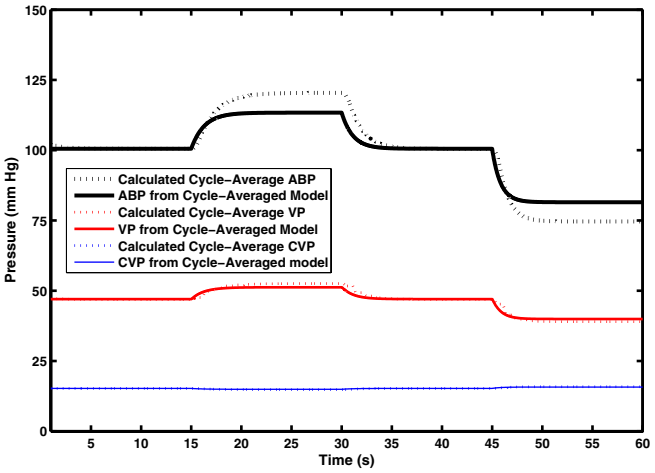

Fig. 6. Transient responses of the index-0 cycle-averaged model for several step changes in peripheral resistance R_3. At t=15 s, R_3 was stepped up to 1.4 units, at t=30 s, R_3 was stepped down to 1 unit, and at t=45 s, R_3 was stepped down to 0.6 units.

model for T=1, during three step changes in systemic vascular resistance R_3: at t=15 s, R_3 was stepped up to 1.4 units; at t=30 s, R_3 was stepped down to 1 unit; and at t=45 s, R_3 was stepped down to 0.6 units. These values of R_3 are on the order of 30-40% of the largest deviations expected in humans. In Fig. 6, the index-0 cycle-averaged model responses are compared to the calculated index-0 cycle-averages from the pulsatile model. The maximum error in the steady-state cycle-averaged waveforms for the ABP, VP, and CVP, was approximately 9%, which is acceptable for the applications we have envisioned for this model.

VI. Conclusion

In this paper, we applied a cycle-averaging method to a simple pulsatile cardiovascular model to derive a cycle-averaged model for cardiovascular dynamics. In ongoing work, we are applying this cycle-averaging methodology to more complicated models of cardiovascular dynamics, with the aim of modularly combining our index-0 cycle-averaged model with more index-0 cycle-averaged compartments to form a larger index-0 cycle-averaged model. The inclusion of feedback control loops around the index-0 cycle-averaged model will also be tackled.

Acknowledgments

This publication was made possible by Grant Number 1 RO1 EB001659 from the National Institute of Biomedical Imaging and Bioengineering. Its contents are solely the responsibility of the authors and do not necessarily represent the official views of the NIBIB or the National Institutes of Health. The authors also wish to thank Dr. Thomas Heldt and Carlos Renjifo for comments on the work and the paper.

References

[1] G. C. Verghese, *Dynamic modeling and control in power electronics*, pp. 1413–1424. The Control Handbook, Boca Raton: IEEE Press, 1996.

[2] T. Heldt, J. L. Chang, J. J. S. Chen, G. C. Verghese, and R. G. Mark, "Cycle-averaged dynamics of a periodically driven, closed loop circulation model," *Control Engineering Practice* vol. 13, no. 9: pp. 1163–1171, 2005.

[3] T. L. Davis and R. G. Mark, "Teaching physiology through interactive simulation of hemodynamics," in *Proceedings of the IEEE Computers in Cardiology*, pp. 649–652, September 1990.

[4] H. Senzaki, C. H. Chen, and D. A. Kass, "Single-beat estimation of end-systolic pressure-volume relation in humans," *Circulation*, vol. 94, pp. 2497–2506, 1994.

[5] T. Heldt, *Modeling of the cardiovascular response to orthostatic stress.* PhD Thesis, Division of Health Sciences and Technology, MIT, September 2004.

[6] V. A. Caliskan, G. C. Verghese, and A. M. Stankovic, "Multi-frequency averaging of dc/dc converters," *IEEE Transactions on Power Electronics*, vol. 14, pp. 124–133, January 1999.

[7] G. P. Tolstov, *Fourier Series*. Dover Publications, Inc, 2nd ed., 1976. Translated by R. A. Silverman.